Measurement Uncertainty in Network Analyzers: Differential Error DE Analysis of Error Models Part 7: Remarks on the Uncertainty Notions -from Lab VNA to Toy NanoVNA-

N.I. Yannopoulou, P.E. Zimourtopoulos

Antennas Research Group, Austria - www.op4.eu

Abstract

From A Common User's Point Of View [FACUPOV] any Vector Network Analyzer [VNA] -from the most expensive Laboratory VNA [Lab VNA] to an extremely cheap Do It Your Self [DIY] NanoVNA [Toy NanoVNA]- that can deliver all the values of its Calibration and the Device Under Test [DUT] in each one of the measurement frequencies, subjects to the uniquely existing estimation of its Measurement Uncertainty in that frequency, that is the one which is computed after the Exact Formation of its Complex ρ-DER Differential Error Region, as well as, of its two Real Differential Error Intervals in polar -rather than rectangular- form: ρ-magnitude DEI and ρ-phase DEI. However, due to the fast and wide spread through the Internet of a huge bunch of accompanying instructions regarding these matters, confusion has arisen from some of the concepts and notations commonly in use in VNA literature which reappears now again, as they are given obscurely, ambiguously, or even incorrectly. Accordingly, this paper presents in full details now, the work done by the authors and announced in the past during the meetings of the circle members of Automatic Network Analyser Metrology [ANAMET] technology group of National Physical Laboratory [NPL] so as to isolate among the also observed then misconceptions, those that definitely require reformulation of their expressions and perhaps a broader consensus on the range of their values and among them primarily that of phase or argument. In addition, in order to highlight the unprecedented advantages of the full and correct computation of DERs and DEIs, the following Practical Applications are included: (a) a comparison between several different in concept and form VNA quantities, (b) a counter example based on previous authors' work, (c) a 3D representation of complex ρ-DERs, and (d) a selected num-

ber of characteristic frames of AVI videos that produced by the authors to show the evolution of the 2-D outline of Complex ρ-DERs and of its two Real ρ-DEIs, both rectangular and polar, uncertainty width in terms of frequency, while the internet links to all of these videos are also provided.

Keywords

Microwave measurements, network analyzer, differential error region, differential error interval, calibration

Introduction

Some useful remarks on the uncertainty notions used in VNA measurements, that we had in mind when we began our research for the systematic errors about 30 years ago, and which came up again after the presentation of the 33rd (Rohde & Schwarz, Fleet, 11 May 2010) and 34th (National Physical Laboratory, Teddington, 21 October 2010) ANAMET meetings and reappeared nowadays are presented here. The unclear and not well defined concepts are mainly due to the fact of introducing the complex numbers to represent the VNA measurements since we measure magnitude and phase. Thus, our first concern is to give a well formed formula for the phase determination of a complex number. Then we examine the information given in relevant literature, old and new, about the phase and its uncertainty, and how it can lead to misunderstandings. A comparison for the magnitude and phase uncertainty is given, with the help of some AVI videos for two different DUTs, a 50-Ohm dc-resistance box as a well closed DUT and a ground plane antenna as an open DUT, of which some representative and notable frames are illustrated.

The merits of using total differentials to determine the measurement uncertainty are discussed and the size of the problem for a numerical evaluation of ΔS_{ij} in one-port and two-port measurements is exposed.

A counter example from an already published authors' work is used in order to demonstrate that a full one-port SLO calibration may not always be considered as a preferable one over that of just a short response S calibration. A 3-D representation of the reflection coefficient together with the DERs as beads around its curve in space is given.

A final remark concerns the use of terms magnitude and amplitude for the value -

size of the involved quantities and the terms argument and phase for the angle. Magnitude is usually used for vectors and amplitude for complex numbers in ac signals or waves, such voltage or current. Argument is used more commonly for complex numbers while phase for sinusoidal functions and waves and it is the most preferable term in general. In the rest of the text the use and meaning both of these two couples are considered from the same view point, although, at least our VNA, definitely use the terms magnitude and phase for what it measures as S_{ij} "vectors" [1]. However, there is a lot of misleading information on the internet and elsewhere about the definition of these quantities. Typically we mention here the case: "Degrees are almost universally used for the phase angles in sinusoidal functions, as in, $\sin(\omega t + 30^{o})$. (Since ωt is in radians, this is a case of mixed units.)".

The first announcement of the present work was a twenty minute presentation in the 35th ANAMET meeting of the National Physical Laboratory [NPL] in 20 October 2011 in Teddington, which is available in

www.antennas.gr/anamet/35/

All the AVI videos produced in order to enhance the presentation of the subject are available as FLOSS in the same link, as above.

On the Notion of Phase

The well-known representation of a complex number $\dot{z}$, with the dot above the character z to clearly signifying its complex nature, in Cartesian and Polar form, is shown in Fig. 1 and defined as

$$\dot{z} = x + i\,y = z\,\angle\hat{\dot{z}},$$
$$z = \sqrt{x^2 + y^2},\ \hat{\dot{z}} \in (-\pi,\ \pi] \qquad (1)$$
$$x = z\cos(\hat{\dot{z}}),\ y = z\sin(\hat{\dot{z}})$$

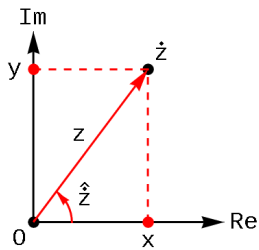

Fig. 1: Complex number

The use of arctangent ($\tan^{-1}$) function to determine $\hat{\dot{z}}$ as a function of one variable is inadequate since it returns wrongly the same argument for opposite complex numbers, red and black points shown in the unit circle in Fig. 2, that is, for complex numbers lying in the first and third (I, III) and in the

second and fourth (II, IV) quadrants and returns values only between $-\pi/2$ and $+\pi/2$ and not in the whole interval of $\hat{z}$, as given in (2),

$$\hat{z} = \tan_p^{-1}\left(\frac{y}{x}\right), \qquad (2)$$
$$(-\infty, +\infty) \rightarrow \left(-\frac{\pi}{2}, +\frac{\pi}{2}\right)$$

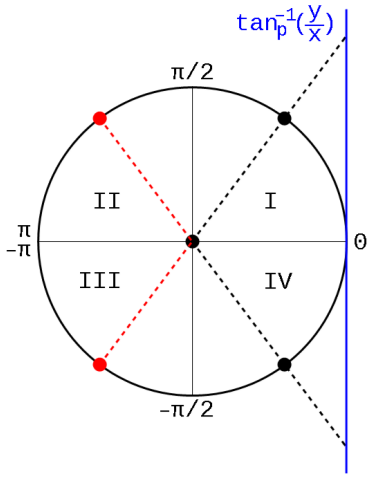

Fig. 2: Arctangent result

It is most appropriate to use the arctangent function of two variables, as defined: a) by taking into account the sign of the real and imaginary part, that is, in which quadrant lies the complex number and b) in terms of the arctangent function of one variable. This function, (3), will return the correct $\hat{z}$ values in the entire interval $(-\pi, \pi]$, as it is expected for complex numbers. Fig. 3 and Tab. 1 give a phase example for nine (9) characteristic points in the unit circle.

$$\mathrm{sgn}(y) = \{y < 0: -1,\ y \geqslant 0: +1\}$$

$$\hat{z} = \tan_2^{-1}(y, x) =$$

$$= \begin{cases} \tan_p^{-1}\left(\frac{y}{x}\right), & x > 0 \\ \mathrm{sgn}(y) * \pi + \tan_p^{-1}\left(\frac{y}{x}\right), & x < 0 \\ \mathrm{sgn}(y) * \frac{\pi}{2}, & x = 0 \\ \frac{0}{0}, & x = 0,\ y = 0 \end{cases} \qquad (3)$$

$$(-\infty, +\infty) \times (-\infty, +\infty) \rightarrow (-\pi, +\pi]$$

In Fortran there is the special function ATAN2 and in Mathematica Arg[z] that automatically produce these values, except for the case x = 0, y = 0 of course.

On the Notion of Phase Uncertainty

1. The first available information on VNA measurements was the very helpful notes of a Vector Seminar by Hewlett-Packard Company [HP] itself in 1989 [2]. As any other printed textbook that can not be changed afterwards, careful study was needed.

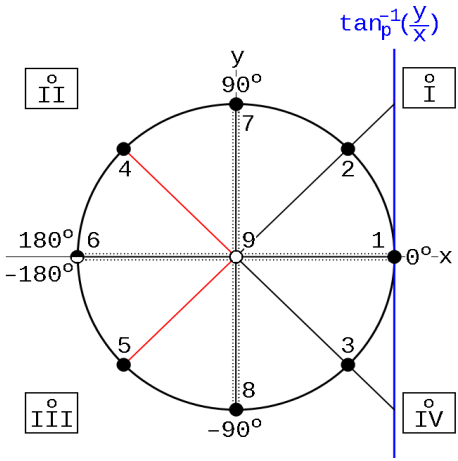

Fig. 3: Phase example - 9 points in unit circle

$$\hat{z} \in \left(-\pi, -\frac{\pi}{2}\right) \cup \left\{-\frac{\pi}{2}\right\} \cup \left(-\frac{\pi}{2}, 0\right) \cup \{0\} \cup \left(0, \frac{\pi}{2}\right) \cup \left\{\frac{\pi}{2}\right\} \cup \left(\frac{\pi}{2}, \pi\right) \cup \{\pi\}$$

Tab. 1: 9 points in unit circle

Point	x	y	$\tan_p^{-1}(y/x)$	$\tan_2^{-1}(y/x)$
1	1	0	0°	0°
2	1	1	45°	45°
3	1	-1	-45°	-45°
4	-1	1	-45°	135°
5	-1	-1	45°	-135°
6	-1	0	0°	180°
7	0	1	∞	90°
8	0	-1	∞	-90°
9	0	0	"0/0"	"0/0"

Thus, in page 3-11 the figure and its adjacent paragraph, shown in Fig. 4, is given, as well as the expressions of Δφ, as phase uncertainty, inside the slide and of ΔS_{11} for the one-port error model of Fig. 5(a), as they appear in the same Seminar notes. Fig. 5(b) shows the one-port error model as it is used in all of our work, with the reflection coefficient ρ of the DUT as it results after calibration and measurement. Noticeable there is a slightly different notation in the same slide used in the Seminar notes between the figure and the relation below it. However there is an obvious correspondence between the involved quantities as: D and E_D of HP with our D, S_{11M} of HP with our m, M_S and E_S of HP with our M, $1+T_R$, E_R of HP with our R, and S_{11A} or S_{11a} of HP with our ρ.

Fig. 4 is very interesting since it includes two (2) inconsistencies, one (1) query and one (1) error, as it is explained step-by-step below.

Step 1 - 2 Inconsistencies: In Fig. 6, at the two yellow marked phrases there is a clear reference at S_{11} after calibration which corresponds to S_{11A} not to S_{11M} which is the measured value. But in the Δφ expression we found the unexpected S_{11M}.

Step 2 - 1 Query: If "ΔS_{11} is perpendicular to the value of S_{11A}", as it is shown in Fig. 7, then the given expression of arc sinus is correct. The question is: is there any case for this statement to be true, and if it is then when it happens.

Step 3 – 1 Error: In Fig. 8 the statement that this is the worst case is wrong, since the worst case, that is, the one which gives the maximum Δφ, results only when we consider the tangent to the circle centered at S_{11A} with radius ΔS_{11}. That means, that the worst case for Δφ will be when ΔS_{11} is perpendicular to the S_{11M} value and not to S_{11A}. We built the [DELTAPHI.AVI] video in order to reveal the wrong statement. Six frames are shown in Fig. 9, for random points on the circle. All frames contain the actual worst case and the case indicated incorrectly as the worst. The variable is the position around the circle centered at S_{11A} with radius the value of ΔS_{11}. Therefore, for every point on the periphery the Δφ angle is outlined with blue color and its value is noted in degrees. The angle for the case of Fig. 8, that is, when ΔS_{11} is perpendicular to S_{11A}, as it is stated in the Seminar notes, is sketched out with green color and its value is written, Fig. 8(c).

The actual worst case is outlined with red color in Fig. 8(e), that is, when S_{11M} is on the tangential line and there is a 90° angle with ΔS_{11}. Since 28.1° > 25.2° the statement under discussion is obviously wrong.

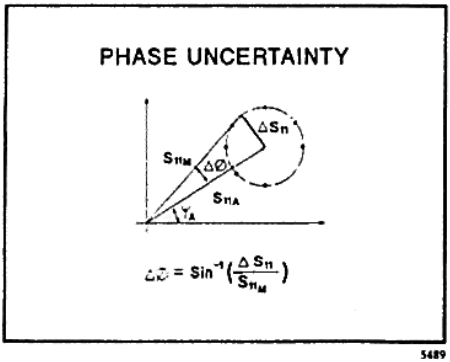

What about phase uncertainty? Phase uncertainty is a function of both s_{11} (the result after calibration) and Δs_{11}. The worst case phase error occurs when Δs_{11} is perpendicular to the value of s_{11a}. Since Δs_{11} is a worst case value, $\Delta\varphi$ which is defined as the arcsin of $(\Delta s_{11}/s_{11})$ is the worst case phase uncertainty about s_{11}.

3-11

$$\Delta S_{11} = S_{11M} - S_{11A} \cong D + T_R\, S_{11A} + M_s\, S_{11A}^2$$

Fig. 4: Phase uncertainty $\Delta\varphi$ and ΔS_{11} [2]

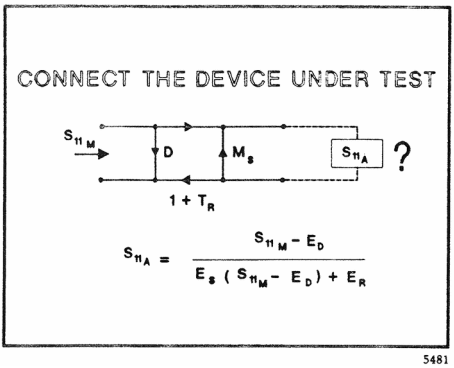

(a) HP Seminar notes

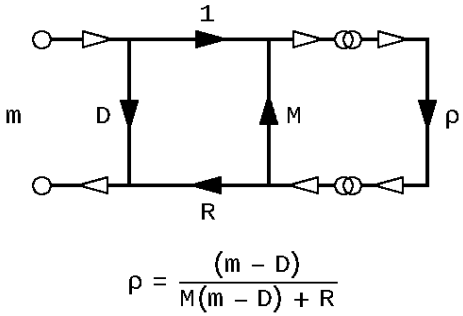

(b) Author's

Fig. 5: One-port error model

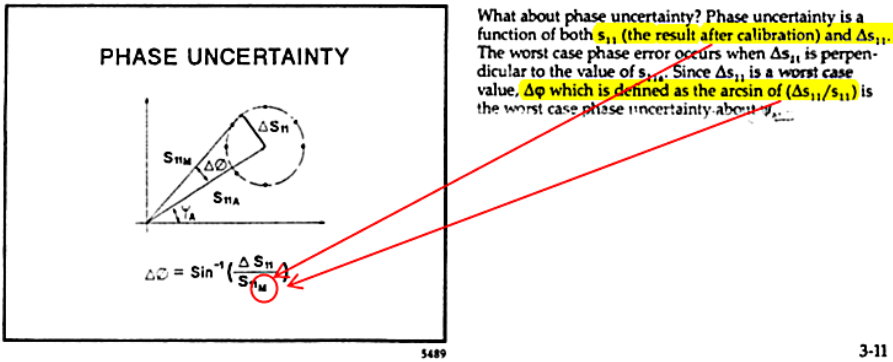

Fig. 6: Two (2) Inconsistencies

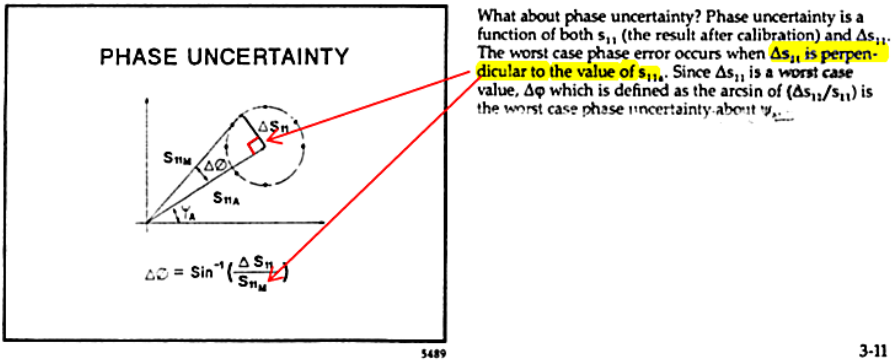

Fig. 7: One (1) Query

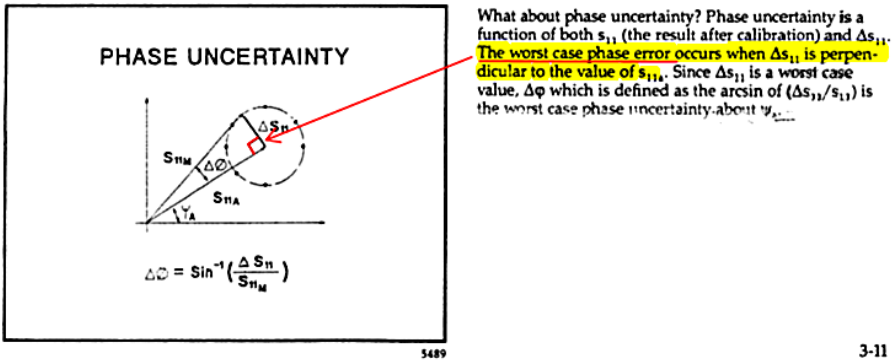

Fig. 8: One (1) Error

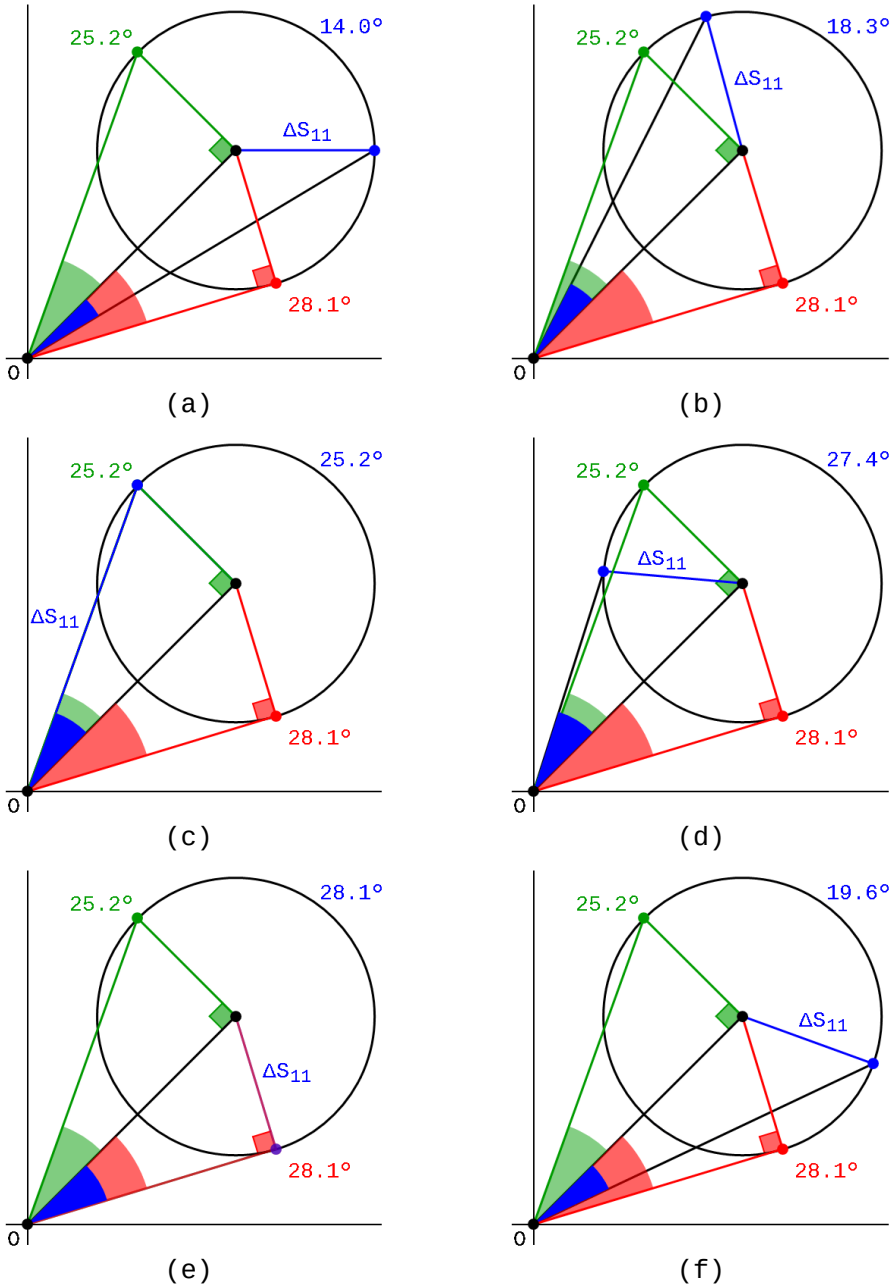

Fig. 9: Six characteristic frames for Δφ values

2. Another issue has to do with the adopted interval of values for phase and its uncertainty. For example, in a presentation of 33rd ANAMET meeting [3], there is a figure showing the phase versus frequency covering the range of values [–5000°, 1000°], while the following, right after that, calculation of electrical length requires the phase to be in radians.

In a presentation of 34th ANAMET meeting [4], an example exists for the reflection coefficient of Thru showing: (1) the linear magnitude with uncertainty greater or equal to 0 and omitting the negative values, (2) the phase is given in the interval (–π, π], while (3) its uncertainty is in the interval (–2π, 2π].

Finally, a presentation of the same ANAMET meeting, as and its corresponding previously published paper [5, 6], shows S_{11}, S_{22} "reflection phase" for a 17 mm air line in the range of –2500° to 0°, which means: six (6) times around the circle plus 340°.

3. Since we basically have ratios and products of complex numbers S_{ij} to deal with, we are interested in difference and addition of phase angles. If we accept the (–π, π] interval from (1) for any phase angle, then obviously the difference of two phase angles will be in the interval (-2π, 2π) and the addition will be in (-2π, 2π]. These intervals cover the unit circle for determining the phase more than once, thus destroying the "1-1" correspondence.

The shape of the correspondence for both difference and addition in the above mentioned intervals is shown in Fig. 10(a) in a Cartesian plot, where the principal interval is indicated by the thick black frame. Fig. 10(b), (c) shows its right and left extension respectively, where we have taken care to keep the same 360° range as in the principal interval. The values of angles that are not included are indicated with an open circle. It is clear that in each of these two intervals there is a discontinuity described by the shown jigsaw function. Moreover, the φ principal angles result from different φ_i value, for example quadrant I results from the interval (0°, 90°) and also from the interval (–360°, –270°). In both figures the number of each quadrant is shown for both axes.

In order to correctly compute the complex number we discriminate two cases: (i) if $\varphi_i \in (-360°, 360°)$ then we use the relations:

$$\varphi = \begin{cases} \varphi_i + 360^\circ, & \varphi_i \le -180^\circ \\ \varphi_i - 360^\circ, & \varphi_i > +180^\circ \\ \varphi_i, & -180^\circ < \varphi_i \le 180^\circ \end{cases} \quad (4)$$

and (ii) if the angle is outside the interval (–360°, 360°) then a two step procedure is needed: (ii.1) we apply the well known Euclid's division lemma extended to negative dividend or negative divisor to find the signed reminder φ_i in (–360°, 0°), or (0°, 360°) as shown in Fig. 10(b), (c) respectively,

$$\varphi' = k\,360^\circ + \varphi_i,\ k \in \mathbb{Z} \quad (5)$$

and (ii.2) apply (4) for φ_i.

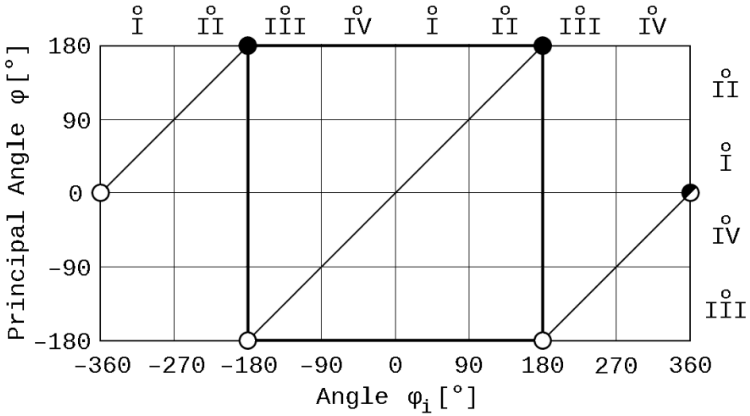

(a) Jigsaw function

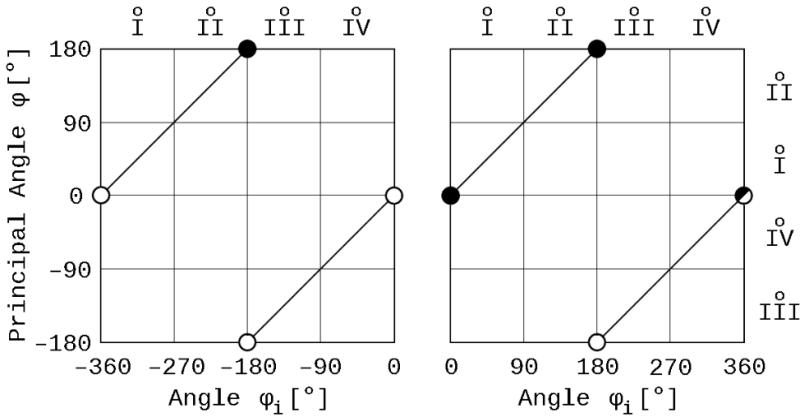

(b) $\varphi_i \le -180^\circ$ (c) $+180^\circ < \varphi_i$

Fig. 10: Principal angle φ in terms of angle φ_i

In order a) to reveal the problem, and b) to amplify our thesis regarding these issues, two extreme examples are presented in Fig. 11. The phase difference of blue point A with phase +177°, in respect to –177° phase of the blue point A' ($\dot{z}_A/\dot{z}_{A'}$), is not 354° but –6°, while the phase difference of red point B with phase –80° in respect to +130° phase of red point B' ($\dot{z}_B/\dot{z}_{B'}$), is 150° and not –210° as:

$\Delta\varphi' = 177° - (-177°) = 354° \Rightarrow$

$\Delta\varphi' > 180° \Rightarrow \Delta\varphi = 354° - 360° \Rightarrow$

$\Delta\varphi = -6°$ and

$\Delta\varphi' = -80° - (+130°) = -210° \Rightarrow$

$\Delta\varphi' < -180° \Rightarrow \Delta\varphi = -210° + 360° \Rightarrow$

$\Delta\varphi = 150°$

Finally, if we consider, as last example, the value –2400° then from (5) we take:

$\varphi' = -2400° = -6 \times 360° - 240°$

and thus from (4):

$\varphi_i = -240° < -180° \Rightarrow$

$\varphi = -240° + 360° \Rightarrow \varphi = 120°$

Notably, there are various ways to use (4) and (5) in practice, because the programming language in use may implement differently the functions integer and fractional parts of a real number.

It is important to keep always in mind what a Vector Network Analyzer, as our HP8505A, can measure and present as indications in [degrees]. Thus, for S_{ij} measurements the range for phase is ±180° [7], as it corresponds to complex numbers, while this range may be different for measurements concerning the electrical length where also the final purpose is different, as occurred in the first ANAMET presentation above [3].

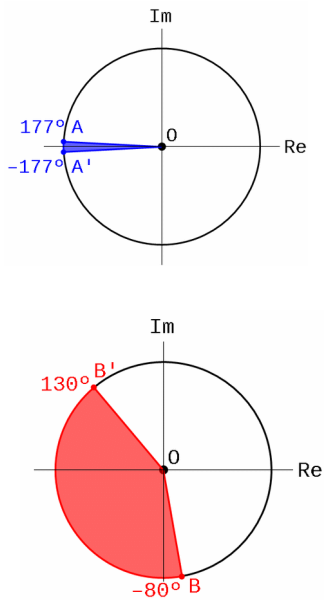

Fig. 11: Extreme Δφ examples

On the Concepts of Magnitute and Phase Uncertainties

The full presentation of our exact estimation of VNA measurement uncertainties in comparison with the approximate ones by HP [2] begins with the contents of Tab. 1. This table contains the various expressions used for the magnitude and phase uncertainties under discussion. In the first row the ΔS_{11}, $\Delta\varphi$ in black print are the expressions produced by HP [2] and reproduced here in Fig. 4, where the used ≅ symbol implies some undeclared there [2] sort of approximations. In the second row, the ΔS_{11}^{F}, $\Delta\varphi^{F}$ are the full -not approximated- expressions produced by us and resulting from the complex difference S_{11M}-S_{11A}, where in dark gray print are the additional terms, which are missing from the corresponding HP expressions [2], above. In the third row, the ΔS_{11}^{d} and $\Delta\varphi^{d}$ in light gray print are correspondingly the absolute value of the difference between the complex numbers $\dot{S}_{11M}$, $\dot{S}_{11A}$ and the phase difference between them. Finally, in the fourth row in red print are shown the defined by us polar DEIs, differential error intervals, for the magnitude and phase of S_{11}.

Two related examples are shown in Fig. 12 and Fig. 13: the first for a Box surround a 50 Ohm dc resistance, and the second for a UHF Ground Plane Antenna (GPA) [8]. Blue color is used for the Differential Error Region (DER) and green for the rectangular DEIs, real and imaginary part. The numeric evaluation of ΔS_{11} results $2^{(7x2)} = 2^{14} = 16{,}384$ points from N = 7 (7 complex variables) interval endpoints, as it was explained in detail in [8, 9].

Almost all of ΔS_{11} points belongs to S_{11}-DER for the selected frequency frames for both these DUTs. ΔS_{11} underestimates the systematic error for the first and overestimates the error for the second. All the corresponding values for magnitude and phase, and their uncertainty are given in Tab. 2, colored accordingly. For the Box it is obvious that the full expression of ΔS_{11} does not give a different result, but for the antenna there is some difference. The DEIs are given in absolute value.

Two AVI videos were produced covering the measured frequency range: 1) [Box-DERs-DEIs.AVI] and 2) [GPA-DERs-DEIs.AVI]. Eight frames were selected for each DUT shown in Fig. 14 (28, 80, 301, 444, 600, 782, 990, 1211 MHz) and Fig. 15 (600, 652, 700, 800, 816, 856, 900, 1000 MHz) re-

spectively, with all the corresponding values with their colors above each frame.

For the 50-Ohm Box a notable case occur at the lowest frequency of 2 MHz where the reflection coefficient S_{11} is nearly 0. The same behavior is true for the next 4 frames, that is, for 15, 28, 41 and 54 MHz. In Fig. 14(a), the results for 28 MHz are shown with the orange point to correspond to the origin O of the coordinate system. ΔS_{11} is very small (black/grey color), while this is a special case for our DER which contains the origin O and it gives a circle for the polar DEIs, as it is already explained in [10, 11].

Tab. 1: Magnitude and phase uncertainty expressions

Magnitude	Phase
$\Delta S_{11} = S_{11M} - S_{11A} \cong D + T_R S_{11A} + M_S S_{11A}^2$	$\Delta\varphi = \sin^{-1}\frac{\Delta S_{11}}{S_{11A}}$
$\Delta S_{11}^F = S_{11M} - S_{11A} = \frac{D + T_R S_{11A} + M_S S_{11A}^2 - DM_S S_{11A}}{1 - M_S S_{11A}}$	$\Delta\varphi^F = \sin^{-1}\frac{\Delta S_{11}^F}{S_{11A}}$
$\Delta S_{11}^d = \lvert \dot{S}_{11M} - \dot{S}_{11A} \rvert$	$\Delta\varphi^d = \hat{\dot{S}}_{11M} - \hat{\dot{S}}_{11A}$
DEI: ΔS_{11}^-, ΔS_{11}^+	DEI: $\Delta\varphi^-$, $\Delta\varphi^+$

Tab. 2: Figs. 10 - 11 Magnitude and phase uncertainty

	50-Ohm Box - 873 MHz	GP Antenna - 976 MHz
S_{11}	0.359∠−60.27°	0.593∠−108.39°
$\lvert S_{11}\rvert$	±0.034, ±0.034, ±0.028, (0.040, 0.037)	±0.193, ±0.200, ±0.211, (0.061, 0.055)
$\angle S_{11}$°	±5.45, ±5.47, ±4.52,	±18.97, ±19.72, ±20.52,
	(7.66, 7.72)	(6.57, 6.64)

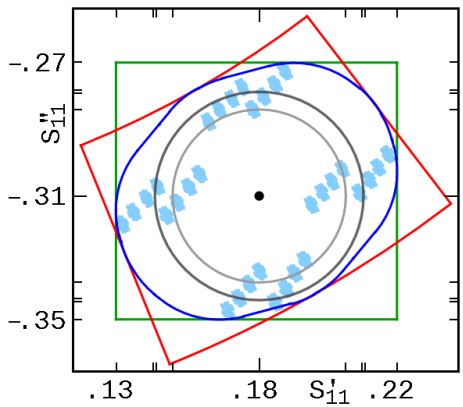

Fig. 12: 50-Ohm Box - 873 MHz

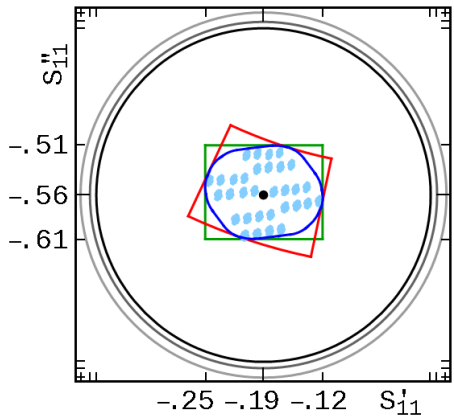

Fig. 13: GP Antenna - 976 MHz

For the antenna: The notable cases are for the frequencies 816, 820, 824 and 828 MHz. For example, at 816 MHz, shown in Fig. 15(e), the orange point of the origin O is inside the ΔS_{11} circle and the arc sinus function cannot give an acceptable answer. At 828 MHz O is exactly on the periphery and still the arc sinus does not work. At 848 (Mag: 0.03, 0.03, 0.25, [0.03, 0.03], Phase: 14.1, 14.1, 142., [15.1, 15.1]) and 856 MHz (Mag: 0.04, 0.04, 0.27, [0.04 , 0.03], Phase: 12.5, 12.6, 98.6, [11.9, 11.8]) shown in Fig. 13(f), the considered errors are comparable, and these are the only cases that this occurs.

The ΔS_{11} numeric evaluation in $2^{(7x2)} = 2^{14} = 16{,}384$ points, took ~5 min on a Netbook Atom N270/1.6GHz,1GB within Mathematica. The numeric evaluation of ΔS_{21} for two-port measurements, demands: $2^{(22x2)}$ = ~18x10^{12} points; at least: $2^{(20x2)}$ = ~1x10^{12} points, if we exclude the Ex crosstalk system error [12]. So, we prepared the mini super computer of Fig. 16, an equivalent to 3xCray-2 Super Computers, many years ago, with a 16 CPUs Cluster, 8xAMD Athlon X2/240 at 2.8 GHz, 16 GB RAM, in GNU/Linux 64-bit PelicanHPC 2.3.2 operating system [13], to try to evaluate all that points with parallel programming in a cluster.

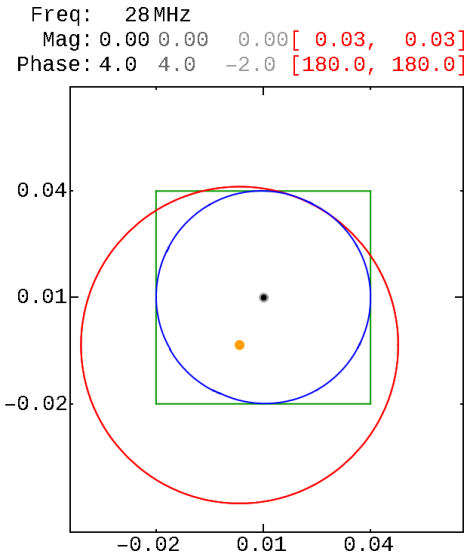
Freq: 28 MHz
Mag: 0.00 0.00 0.00 [0.03, 0.03]
Phase: 4.0 4.0 −2.0 [180.0, 180.0]
0.04
0.01
−0.02
−0.02
0.01
0.04

(a)

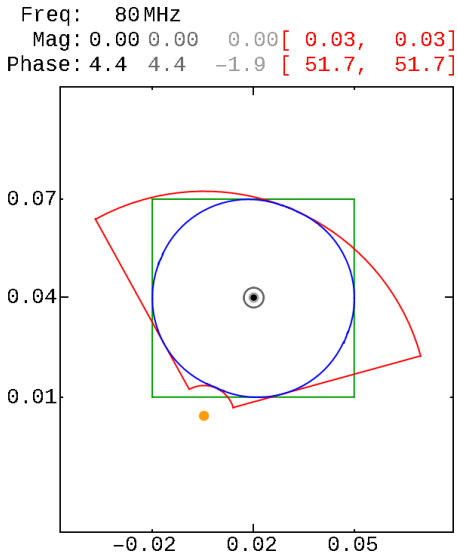
Freq: 80 MHz
Mag: 0.00 0.00 0.00 [0.03, 0.03]
Phase: 4.4 4.4 −1.9 [51.7, 51.7]
0.07
0.04
0.01
−0.02
0.02
0.05

(b)

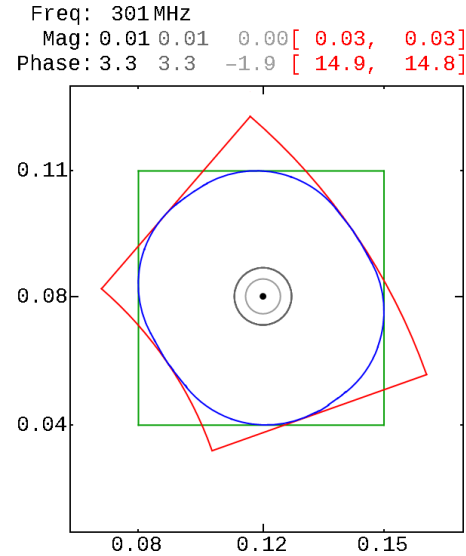
Freq: 301 MHz
Mag: 0.01 0.01 0.00 [0.03, 0.03]
Phase: 3.3 3.3 −1.9 [14.9, 14.8]
0.11
0.08
0.04
0.08
0.12
0.15

(c)

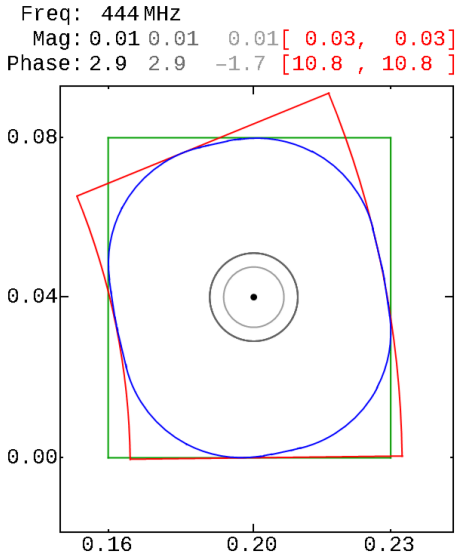
Freq: 444 MHz
Mag: 0.01 0.01 0.01 [0.03, 0.03]
Phase: 2.9 2.9 −1.7 [10.8 , 10.8]
0.08
0.04
0.00
0.16
0.20
0.23

(d)

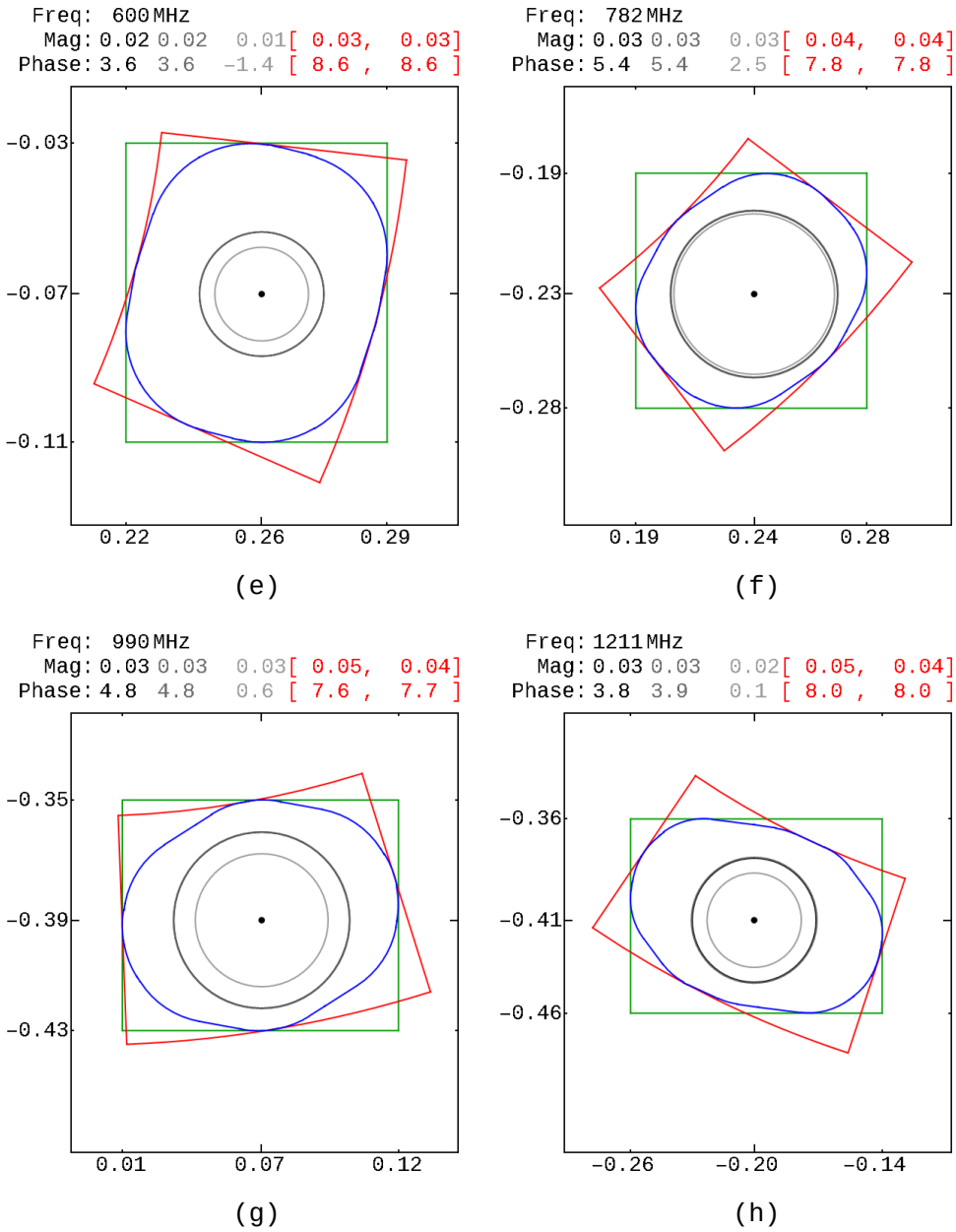

Fig. 14: Characteristic frames from [Box-DERs-DEIs.AVI]

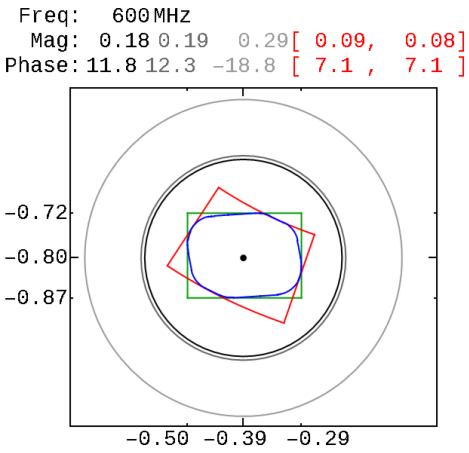
Freq: 600 MHz
Mag: 0.18 0.19 0.29 [0.09, 0.08]
Phase: 11.8 12.3 −18.8 [7.1 , 7.1]
−0.72
−0.80
−0.87
−0.50 −0.39 −0.29

(a)

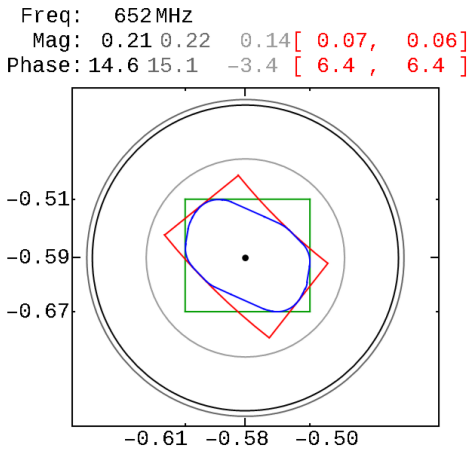
Freq: 652 MHz
Mag: 0.21 0.22 0.14 [0.07, 0.06]
Phase: 14.6 15.1 −3.4 [6.4 , 6.4]
−0.51
−0.59
−0.67
−0.61 −0.58 −0.50

(b)

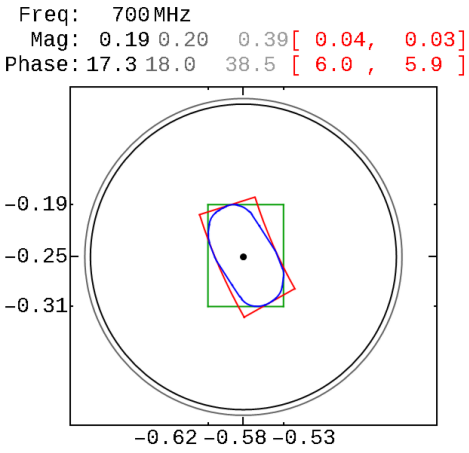
Freq: 700 MHz
Mag: 0.19 0.20 0.39 [0.04, 0.03]
Phase: 17.3 18.0 38.5 [6.0 , 5.9]
−0.19
−0.25
−0.31
−0.62 −0.58 −0.53

(c)

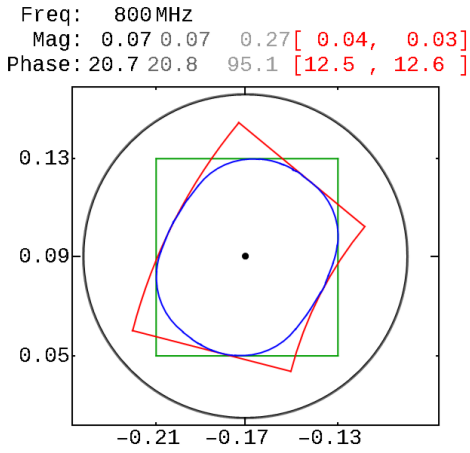
Freq: 800 MHz
Mag: 0.07 0.07 0.27 [0.04, 0.03]
Phase: 20.7 20.8 95.1 [12.5 , 12.6]
0.13
0.09
0.05
−0.21 −0.17 −0.13

(d)

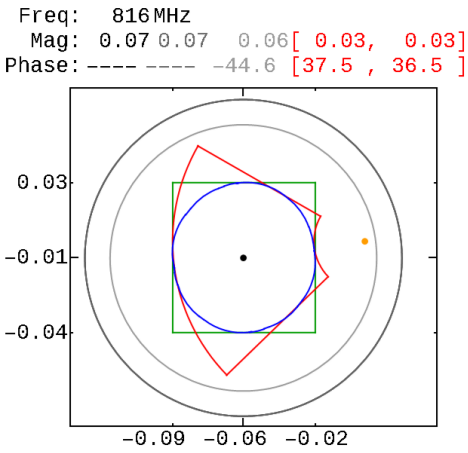

(e)

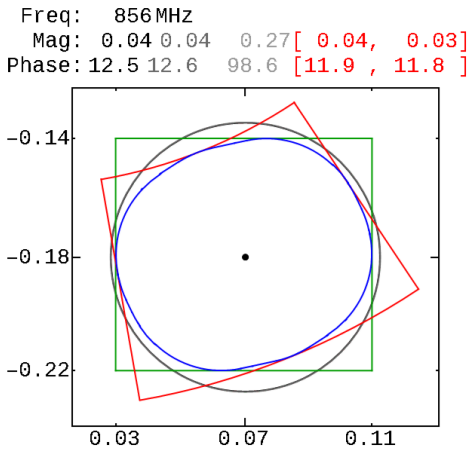

(f)

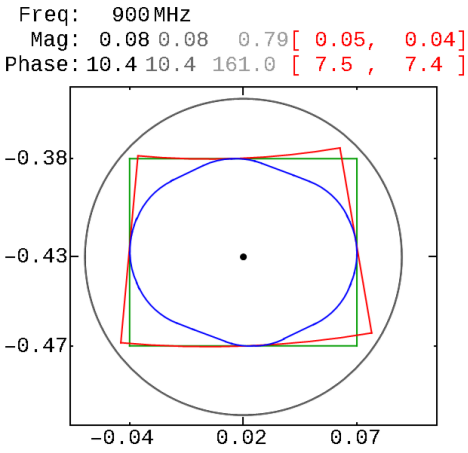

(g)

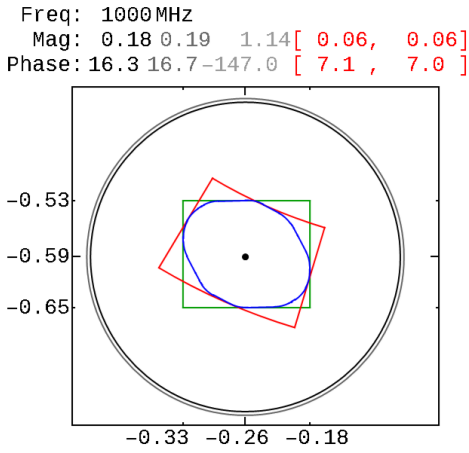

(h)

Fig. 15: Characteristic frames from [GPA-DERs-DEIs.AVI]

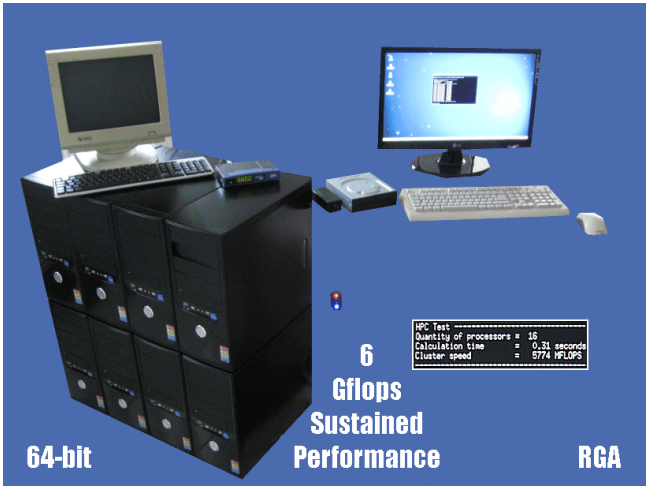

Fig. 16: The RGA mini-Super computer

The Notion of Complex DER

In [14] someone can read for the S-parameters of a two-port error model: "Luckily you don't need to know these equations to use network analyzers". By the same reasoning, and probably to a greater extent, it is not necessary to know the expressions of the total differentials which produce the DERs' points. You need only the software tool in order to evaluate them [10, 11]. Some remarks for total differentials are:

1. Involve Linear relations by default.

2. Result in exact cyclo-polygonal regions in complex plane instead of approximate circles or ellipses.

3. Produce rectangular intervals, DEIs, for real and imaginary parts, and polar DEIs for magnitude and phase.

4. Demand careful use of mathematics.

5. Give answer to special cases.

6. Make possible the expression of interconnection between measurements and instrument specifications.

Another remarkable point for the advantages of total differentials came up during the PhD thesis [15] where a number of 3,059 possible antennas where presented, with 900+ figures, and 436 of them were constructed and measured. The production of three (3)

figures for only one (1) antenna is based on 42,432 measurements and almost 23 hours work with our HP 8505A were needed. And the query is: if a method based on statistical principles was used to determine the uncertainty for this specific antenna characteristics, then how many measurements would be necessary for the same antenna system in order to ensure a valid result? Statistics are simple enough, but time consuming under real conditions. A second query is: What errors do they really include?

A Counter Example

As a counter example to the full one-port calibration we bring back here the case of short response calibration for the reflection coefficient measurement of the UHF ground plane antenna [16]. The paper is open for permanent review at the given link in References below and for details. Fig. 17 shows the transformation of the one-port error model of Fig. 4(b), where the dashed boxes indicate the two system errors, directivity D and source match M, that do not exist.

Fig. 18 shows the comparison of the reflection coeffient after SLO and only S calibration with ρ-DERs and ρ_S-DERs as stripes with light and dark gray color respectively. It is obvious that the two curves are very close, and that the DERs for ρ_S are much smaller. Fig. 19 shows the polar DEIs as stripes for the magnitude and phase of ρ and ρ_S where the ρ_S stripes are inside the corresponding ρ stripes almost in the whole frequency range.

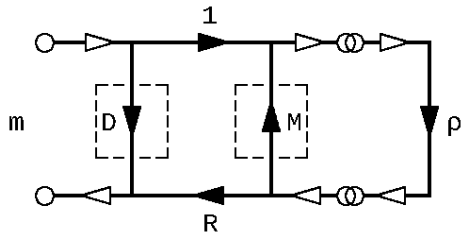

Fig. 17: One-port error model

Numerous results having as follows. Fig. 20 shows the two ρ-DERs after SLO and after S calibration for the selected frequency of 796 MHz, with their DEIs in rectangular and polar form. In Tab. 3 the values for magnitude, phase and their DEIs demonstrate the difference between the results of the two calibration techniques.

In short - response calibration only the R system error can be taken into account and it is given in Fig. 21 for the two calibration techniques in 3-D and 2-D. The black color is used for the full one-port SLO calibration and the red color for the S

short - response calibration. The corresponding R, R_S-DERs for the selected frequency are shown in Fig. 22.

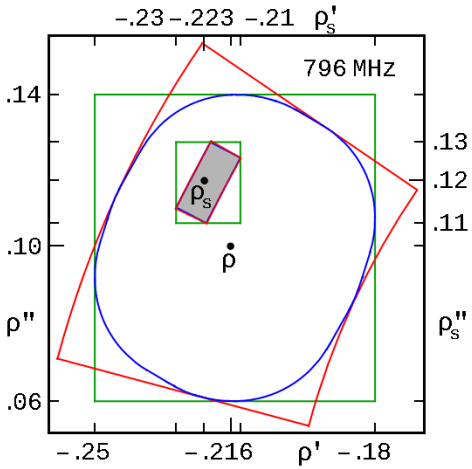

Fig. 20: ρ, ρs DERs and DEIs

Tab. 4 contains the Min, Max and Mean value of the difference for magnitude and phase between the two cases. Obviously the R curve in Fig. 21 is the same but there is a phase difference.

In Fig. 23 ρ and ρs are shown in 3-D with some selected DERs as beads for the two cases. The vertical axis corresponds to frequency from 600 to 1000 MHz. The figure was produced in Mathematica 7 and it was interactive. From this figure we creat the film [3D-DERs-DEIs.AVI] where some views are shown.

This is a counter example for the use of full one-port SLO calibration versus a simple response calibration with just one standard. The paper was uploaded to Agilent forum for open review back in 2011 with subject "Systematic Uncertainties in VNA Measurements" by pez, Total posts: 7, Total Views: 3,400+. We copied a comment which includes at least 5 interesting issues:

"... in older equipment and at low frequencies, where the directional couplers were well match (sometimes better than the loads you could purchase) but not applicable once you move away from the test port through any kind of test cable ...",

by D.J., PhD, Agilent Fellow, Total posts: 1,800+. The inial link of the forum is unfortunately not available any more, but the information has been archived by the authors at their site [17].

These issues need further investigation concerning both the older and the newer equipment for their ability to achieve a certain degree of satisfactorily accurate VNA measurements.

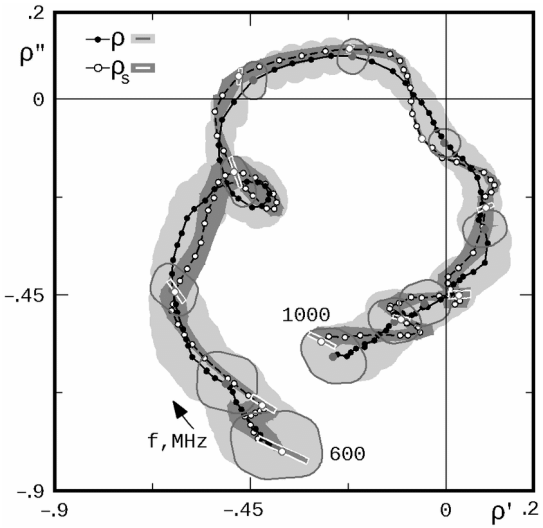

Fig. 18: Complex ρ-DERs and ρs-DERs in [600, 1000] MHz

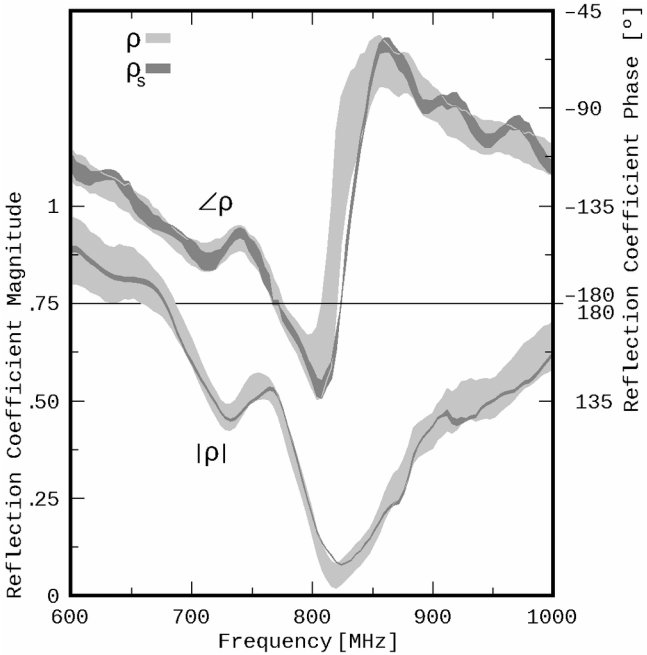

Fig. 19: Polar DEIs of reflection coefficient

Tab. 3: ρ and ρs polar DEIs

ρ = 0.238 ∠155.3°	
|ρ| (0.035, 0.033)	∠ρ (9.60°, 9.73°)
ρs = 0.251 ∠152.4°	
|ρs| (0.006, 0.003)	∠ρs (2.25°, 2.25°)

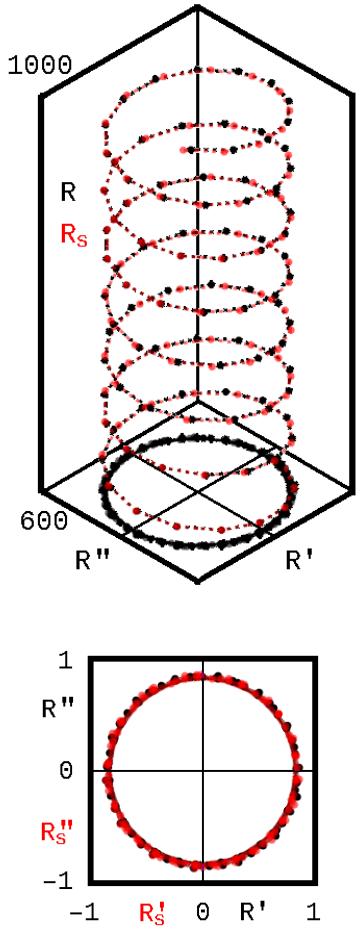

Fig. 21: R, Rs in 3-D and 2-D

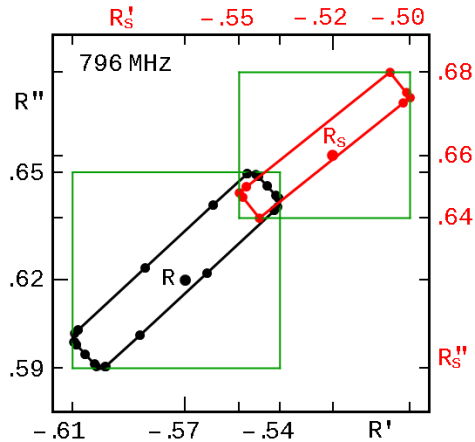

Fig. 22: R-DER, and Rs-DER

Tab. 4: R, Rs differences

600-1000 MHz	Min	Max	Mean
|R| – |Rs|	16×10^{-6}	15×10^{-3}	4.39×10^{-3}
∠R – ∠Rs [°]	0.04	10.61	4.65

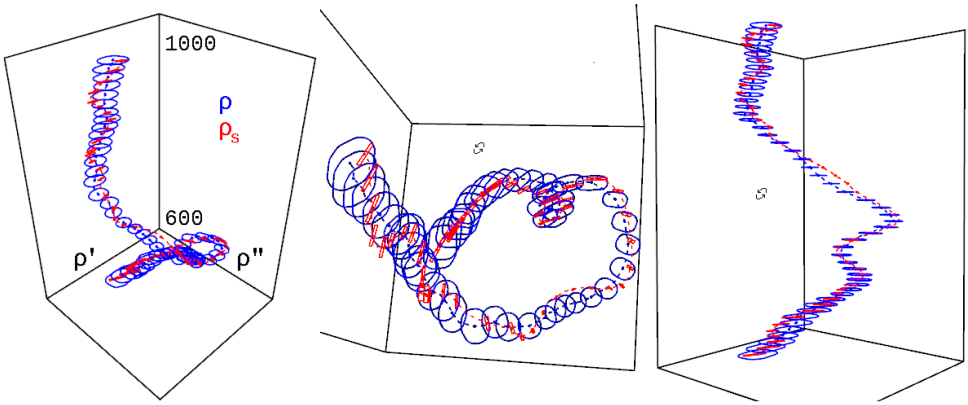

Fig. 23: Complex ρ, ρ_s with selected DERs in [600, 1000] MHz

Conclusion

Due to the one-to-one correspondence between the points of ℂ complex plane and $\mathbb{R}^2$ often the complex numbers corresponding to ordered pairs of real numbers are treated as vectors. This is how the "Vector" designation has been established for the Network Analyzer which measures magnitude and phase. We have tried here to demonstrate the confusion caused by the meaning of the word "phase" at least in relation to measurements of S_{ij} in the frequency domain. We did not deal at all for example with the area of measurements with a VNA related to Electrical Length. We accept the use of the terms Magnitude and Phase imposed by VNA but emphasize that the pairs are in our opinion (Magnitude, Argument) and (Amplitude, Phase), the latter coming closer to physical reality.

We have shown that a hasty and careless reading of the available literature can lead to misunderstandings, and we have compared different ways of calculating the uncertainty in S_{11} reflection coefficient measurement for two loads with the additional visual aid provided by videos. Through these, the variety of different frequency-dependent produced DERs was revealed. Additionally, their 3-D representation provides a complete picture of what one can expect for the behavior of the DUTs we measure, at least the open ones, under real-world conditions.

Some positive points for the advantageous use of our own method of DERs and DEIs

were mentioned and the size of the problem for a direct numerical calculation of ΔS_{ij} was highlighted.

Finally, with a counter-example we showed that there is a case with a simple and fast Short-Response only calibration where it is possible to get the required accuracy for the S_{11} measurements although this conclusion resulted a-posteriori.

However, many issues still exist, as we stated, and require further study.

References

[1] HP 8505A RF Network Analyzer Basic Measurements, Application Note 219, Palo Alto California, November 1978, p. 3

[2] HP, "Vector Measurements of High Frequency Networks", Hewlett-Packard, HP publication number 5958-0387, 1989, pp. 3-9, 3-11

[3] Horibe M., "Verification of VNA reflection phase measurements", 33rd ANAMET meeting, Rohde & Schwarz, Fleet, 10 May 2010 "http://resource.npl.co.uk/docs/networks/anamet/members_only/meetings/33/20100511_anamet33_masahiro.pdf"

[4] Salter M., "Uncertainty in magnitude and phase by analytical propagation of distributions", 34th ANAMET meeting, National Physical Laboratory, Teddington, 21 October 2010 "http://resource.npl.co.uk/docs/networks/anamet/members_only/meetings/34/20101021_anamet34_salter1.pdf"

[5] Hoffmann J.P, Leuchtman P, Ruefenacht J., Wong K., "S-parameters of slotted and slotless connectors", 34th ANAMET meeting, National Physical Laboratory, Teddington, 21 October 2010

[6] Hoffmann J.P, Leuchtman P, Ruefenacht J., Wong K., "S-parameters of Slotted and Slotless Coaxial Connectors", 74th ARFTG Microwave Measurement Conference, 2009, DOI: 10.1109/ARFTG74.2009.5439109 "https://ieeexplore.ieee.org/document/5439109"

[7] HP 8505A Network Analyzer, High Performance RF Network Analyzer, Technical Data, January 1979, Palo Alto California, USA, pp. 14 – 17

[8] Yannopoulou N., Zimourtopoulos P., "Total Differential Errors in One Port Network Analyzer Measurements with Application to Antenna Impedance", Radioengineering, Vol. 16, No. 2, June 2007, pp. 1 - 8 "www.radioeng.cz/fulltexts/2007/07_02_01_08.pdf"

[9] Yannopoulou N.I., Zimourtopoulos P.E., "Measurement Uncertainty in Network Analyzers: Differential Error Analysis of Error Models Part 1: Full One-Port Calibration", FunkTechnikPlus # Journal, Issue 1, Year 1, 2013, pp. 17 - 22 "www.ftpj.otoiser.org/issues/html/ftpj-issue-01-e4-lo4104-pdfc171-ia1.htm" (1-2)

[10] Yannopoulou N.I., Zimourtopoulos P.E., "Measurement Uncertainty in Network Analyzers: Differential Error DE Analysis of Error Models Part 6: FLOSS - Software Tools", FunkTechnikPlus # Journal, Issue 26-27, Year 9, 2022, pp. 7 - 26 "www.ftpj.otoiser.org/issues/html/ftpj-issue-26-27-lo4104-pdfc171-ia1.htm" (26-27-1)

[11] Yannopoulou N.I., Zimourtopoulos P.I., "Complex Differential Error Regions: Software Tools", 31st ANAMET Club Meeting 02/04/2009 "http://resource.npl.co.uk/docs/networks/anamet/members_ only/meetings/31/yannopoulou.pdf" Update 23/09/2019 "www.op4.eu/anamet/31"

[12] Yannopoulou N.I., Zimourtopoulos P.I., "Measurement Uncertainty in Network Analyzers: Differential Error DE Analysis of Error Models Part 5: Step-by-Step Graphical Construction of Complex DE Regions and Real DE Intervals", FunkTechnikPlus # Journal, Issue 16, Year 5, 2018, pp. 7 - 25 "www.ftpj.otoiser.org/issues/html/ftpj-issue-13-16-lo4104-pdfc171-ia1.htm" (13-16-1)

[13] Creel M., PelicanHPC Tutorial, UFAE and IAE Working Papers from Unitat de Fonaments de l'Anàlisi Econòmica (UAB) and Institut d'Anàlisi Econòmica (CSIC) "https://econpapers.repec.org/paper/aubautbar/749.08.htm"

[14] Ballo D., "Network Analyzer Basics", Hewlett–Packard Company, 1998, pp. 58

[15] Yannopoulou N.I., "Study of monopole antennas over a multi-frequency decoupling cylinder", PhD Thesis, EECE, DUTh, February 2008 (in Hellenic), pp. (6-38) - (6-39) "www.didaktorika.gr/eadd/handle/10442/20920?locale=en"

[16] Yannopoulou N.I., Zimourtopoulos P.I., "Measurement Uncertainty in Network Analyzers: Differential Error Analysis of Error Models Part 3: Short One-Port Calibration – Comparison", FunkTechnikPlus # Journal, Issue 2, Year 1, 2013, pp. 41 - 49 "www.ftpj.otoiser.org/issues/html/ftpj-issue-02-e4-lo4104-pdfc171-ia1.htm" (2-3)

[17] Agilent Discussion Forums, "https://www.antennas.gr/anamet/35/Agilent_Discussion_Forums-View_topic-Systematic_Uncertainties_in_VNA_Measurements.htm"

* Active Links: 19.01.2024 - Inactive Links : FTP#J Link Updates: http://updates.ftpj.otoiser.org/